

## Glass-Specific Behavior in the Damping of Acousticlike Vibrations

B. Rufflé,<sup>1</sup> G. Guimbretière,<sup>1</sup> E. Courtens,<sup>1</sup> R. Vacher,<sup>1</sup> and G. Monaco<sup>2</sup>

<sup>1</sup>*Laboratoire des Colloïdes, Verres et Nanomatériaux, UMR 5587 CNRS, Université Montpellier II, F-34095 Montpellier Cedex 5, France*

<sup>2</sup>*European Synchrotron Radiation Facility, Boîte Postale 220, F-38043 Grenoble, France*

(Received 6 June 2005; published 31 January 2006)

High frequency sound is observed in lithium diborate glass,  $\text{Li}_2\text{O}-2\text{B}_2\text{O}_3$ , using Brillouin scattering of light and x rays. The sound attenuation exhibits a nontrivial dependence on the wave vector, with a remarkably rapid increase towards a Ioffe-Regel crossover as the frequency approaches the boson peak from below. An analysis of literature results reveals that the boson-peak frequency is closely related with a Ioffe-Regel limit for sound in many glasses. We conjecture that this relation, specific to glassy materials, might be rather common among them.

DOI: [10.1103/PhysRevLett.96.045502](https://doi.org/10.1103/PhysRevLett.96.045502)

PACS numbers: 63.50.+x, 78.35.+c, 81.05.Kf

Phenomena occurring in glasses near the upper end of acoustic branches are of considerable interest. Indeed, they directly relate to the thermal anomalies of these materials [1] and, ultimately, to their structure on the nanometer scale. Acoustic modes propagate in glasses as in isotropic continua up to frequencies  $\Omega/2\pi$  of several hundred GHz [2]. Their damping mainly has two origins: (i) tunneling or thermally activated relaxation of defect sites [3], and (ii) mode anharmonicity [4]. As  $\Omega/2\pi$  approaches the THz, several additional inhomogeneouslike damping mechanisms have been invoked, such as Rayleigh scattering [5], crystal-like cluster effects [6,7], or resonance with inhomogeneously distributed low-lying opticlike modes [8]. We already reported extensive inelastic x-ray scattering (IXS) observations of Brillouin spectra near the end of the longitudinal acoustic branch on permanently densified silica glass,  $d\text{-SiO}_2$  [9–11]. Particular attention was given to the linewidth  $\Gamma$  obtained from damped harmonic oscillator (DHO) fits of the spectra. A rapid increase in  $\Gamma$  is observed on approaching from below a Ioffe-Regel (IR) crossover at  $\Omega_{\text{IR}}$  [11]. Beyond  $\Omega_{\text{IR}}$ , the modes cease to possess a well defined wave vector  $q$ , strictly implying the end of the “branch”  $\Omega(q)$ . We also found that the acoustic excitations merge then with the boson peak (BP) [10]. The latter corresponds to an excess in the density of vibrational states  $g(\omega)$ . The position of the peak,  $\Omega_{\text{BP}}$ , is defined by the maximum in the reduced density,  $g(\omega)/\omega^2$ . In silica, the excess has a strong opticlike component [12–14]. The relation  $\Omega_{\text{IR}} \simeq \Omega_{\text{BP}}$  implies a resonance of BP modes with acoustic modes near the IR limit. The rather local low-lying optic modes [15] can hybridize with acoustic modes [16,17] producing the IR crossover. It is, of course, crucial to examine to what extent this property is common to glasses. This is the main purpose of the present Letter.

First, we report with all necessary details the rapid increase of  $\Gamma$  upon approaching the IR crossover in a second glass, lithium diborate  $\text{Li}_2\text{O}-2\text{B}_2\text{O}_3$ , or LB2. It is already known that this crossover exists in LB2 [18]. It is also an excellent glass for this experiment. Indeed, we

show below that  $\Omega_{\text{IR}}/2\pi$  is  $\simeq 2.1$  THz (or  $\hbar\Omega_{\text{IR}} \simeq 8.8$  meV) and that the corresponding crossover wave vector  $q_{\text{IR}}$  is  $\simeq 2.1$  nm<sup>-1</sup>. Hence, both are sufficiently high to allow for a meaningful exploration of the approach of  $\Omega_{\text{IR}}$  using current IXS capabilities. The x-ray results are complemented with Brillouin light scattering (BLS), which shows that, in the GHz range,  $\Gamma$  in LB2 is mainly controlled by relaxation. This is contrary to  $d\text{-SiO}_2$ , where similar measurements reveal that  $\Gamma$  is dominated by anharmonicity [19]. We find, however, that the onset of the IR crossover, as well as the behavior in the crossover region, are entirely similar in LB2 and  $d\text{-SiO}_2$ . This indicates that the crossover mechanism is unrelated to the homogeneous broadening at lower frequencies. Further, our results show that the BP of LB2 also corresponds to an excess of modes, and that  $\Omega_{\text{IR}} \simeq \Omega_{\text{BP}}$ . As demonstrated below for both LB2 and  $d\text{-SiO}_2$ , plots of  $\Gamma/\Omega$  vs  $\Omega$  allow one to reliably obtain  $\Omega_{\text{IR}}$ . This encouraged us, second, to extract from the literature on other glasses the information on  $\Gamma$  in the THz range. Although the data are often fragmentary, plots of  $\Gamma/\Omega$  allow one in many cases to obtain meaningful estimates for  $\Omega_{\text{IR}}$ . We find that in all cases  $\Omega_{\text{IR}}$  is closely related to  $\Omega_{\text{BP}}$ .

X-ray Brillouin scattering experiments on LB2 were performed on the high-resolution spectrometer ID16 at the European Synchrotron Radiation Facility in Grenoble, France. The experimental conditions were similar to those described in [11]. Measurements were taken at two temperatures  $T$ , 300 and 573 K. Elevated temperatures are favorable to increase the Brillouin signal by the Bose factor. However, we refrained from nearing the glass transition, as  $\text{Li}^+$  diffusion grows then rapidly [20]. Figure 1 illustrates typical spectra at 573 K and their fits. The indicated values of the scattering vector  $Q$  correspond to the center of the collection slit, which gives a spread  $\Delta Q \simeq \pm 0.18$  nm<sup>-1</sup>. The spectrum in Fig. 1(a) is taken at the smallest usable  $Q$ . It consists of an elastic peak plus a Brillouin doublet. The small constant background, fixed to the known detector noise, is already subtracted. Each such

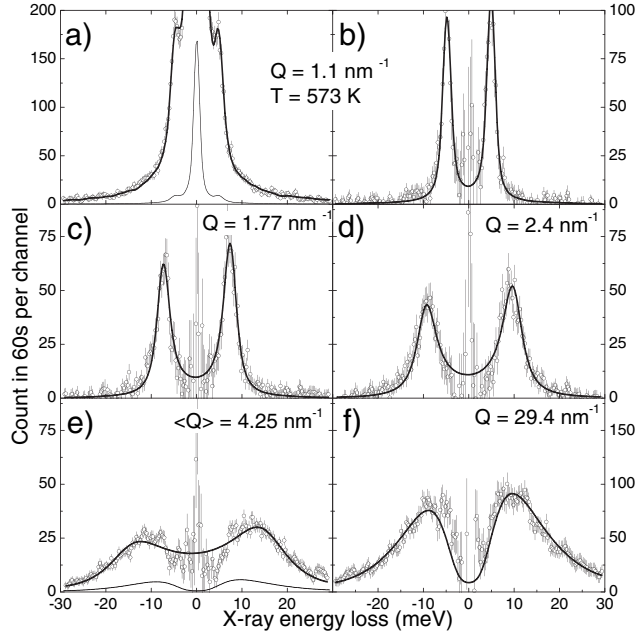


FIG. 1. IXS spectra of LB2 and their fits explained in the text. (a) A full spectrum and its central portion  $\times 1/20$ ; (b)–(e) The inelastic part remaining after subtraction of the elastic component determined in a global fit of each spectrum. The lines show the DHO adjustment in this global fit. (f) The inelastic part of a high- $Q$  spectrum treated in the same manner but adjusted to a log-normal reproducing the BP.

spectrum was adjusted to an elastic line plus a DHO, convoluted with the separately measured instrumental response, taking into account the frequency spread produced by the collection aperture. For clarity, the fitted elastic peak has been subtracted from both the data and the solid line in Figs. 1(b)–1(f), maintaining the original error bars. This just makes the inelastic parts well apparent. The Brillouin width seen in Fig. 1(b) is nearly all instrumental, while it contains a real broadening in Fig. 1(c). The latter becomes the dominant part in Fig. 1(d) for which  $Q \sim q_{\text{IR}}$ , with  $\hbar\Omega_{\text{IR}} \sim 9$  meV as explained below. It is seen that the DHO line shape starts deviating systematically from the measured signal around  $q_{\text{IR}}$ . The spectrum in Fig. 1(e) is actually the mean of four spectra accumulated from 4.1 to 4.4  $\text{nm}^{-1}$ . At these high  $Q$  values the spectra evolve so slowly with  $Q$  that taking a mean is a good procedure for increasing the signal-to-noise ratio. The additional spread in  $Q$  was taken into account in the fit which, however, is then quite poor, showing that the DHO is no more a valid approximation. All these observations are remarkably similar to previous ones on  $d\text{-SiO}_2$ . Figure 1(f) shows a spectrum at 29.4  $\text{nm}^{-1}$  fitted to a log-normal [21]. This is essentially the BP as discussed below.

The parameters extracted from the DHO fits of the IXS spectra are shown in Fig. 2. They exhibit very little dependence on  $T$ , if any. Below the crossover there is only a slight departure from linear dispersion as seen in Fig. 2(a).

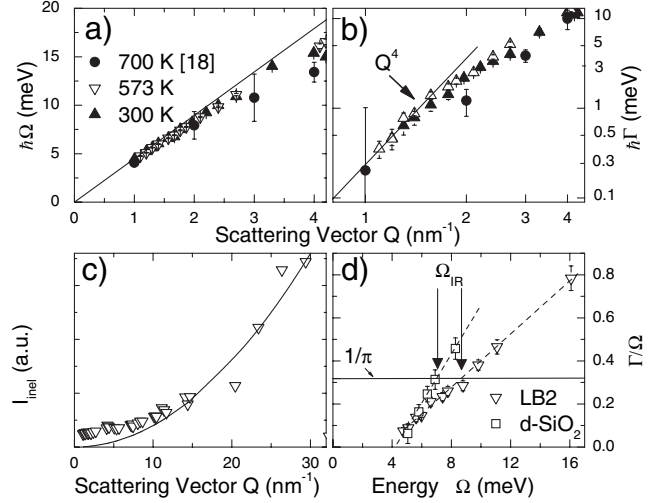


FIG. 2. (a),(b) The parameters of the DHO fits for the two temperatures, 573 and 300 K. The four full dots at 700 K are from [18]. The slope of the line in (a) is the BLS velocity measured independently. In (b) the error bars at 573 K are mostly smaller than the symbols, while these at 300 K (not shown) are about twice as large. The line of slope 4 in (b) is drawn through the first five points at 573 K. (c) The integrated inelastic intensities at 573 K, corrected for the oxygen-ion form factor, with a line  $\propto Q^2$ . (d) The method used to determine  $\Omega_{\text{IR}}$  applied to LB2 (these data) and  $d\text{-SiO}_2$  (data from [11]). The straight lines are guides to the eye. The crossover positions are at the intercept with the ordinate  $1/\pi$ .

In this region one can consider that the experiment detects approximate plane waves with  $q = Q$ . There is, however, a very rapid increase of the full width  $\Gamma$  at the lowest  $Q$  values, as shown in Fig. 2(b). A power law  $Q^4$  has been drawn through the five lowest points at 573 K. A fit to these five points actually gives the power  $4.2 \pm 0.1$ . As can be expected, this rapid increase of  $\Gamma$  saturates as the crossover is approached from below, starting here for  $Q \sim 2 \text{ nm}^{-1}$ . There is then a progressive merging of the sound excitations with the opticlike BP. Although  $Q$  remains fixed by the scattering geometry, the excitations that are observed might then be so far from plane waves that  $q$  becomes ill-defined. The position of opticlike modes is  $Q$  independent, which we have observed in comparing spectra taken at 23.4, 26.4, and 29.4  $\text{nm}^{-1}$ . In the incoherent approximation, their integrated intensity should be proportional to  $Q^2$  [22]. The total inelastic intensity  $I_{\text{inel}}$ , corrected for the atomic form factor of oxygen, is shown in Fig. 2(c). At low  $Q$ , the Brillouin signal contributes a constant. The  $Q^2$  dependence is seen at high  $Q$ , confirming that Fig. 1(f) shows mainly the scattering from the BP, whose shape actually agrees with Raman scattering [23]. Extrapolating the intensity of the log-normal shown in Fig. 1(f) to the  $Q$  value of Fig. 1(e) leads to the thin line drawn there. This is only a small fraction of the spectral intensity, so that what is seen in Figs. 1(b)–1(e) is mostly produced by acoustic-like excitations, while at higher  $Q$  these merge into optic-

like modes. A similar merging of the acoustic mode into the BP was observed in  $d$ -SiO<sub>2</sub> [10]. Incidentally, we also show in Figs. 2(a) and 2(b) the four data points from the previous measurement at 700 K [18]. Besides a slight quantitative difference, it is obvious that there is insufficient information to allow for the present discussion.

It remains to determine  $\Omega_{\text{IR}}$ . The exact location of the IR limit is a matter of definition. We place the crossover at the frequency where the *energy* mean free path of sound first reaches down to half its wavelength,  $\ell = \lambda/2$ . The exponential decay model leading to the DHO gives  $\ell^{-1} = \Gamma/v$ , where  $\Gamma$  is in rad/s and  $v = \Omega/q$  is the sound velocity. With  $q = 2\pi/\lambda$ , this leads to the crossover criterion  $\Gamma = \Omega/\pi$ . Although a peak in the DHO spectrum is still clearly identified for  $\Gamma = \Omega/\pi$ , one recognizes that a plane wave whose energy decays by a factor  $1/e^2$  over a wavelength corresponds well to the concept of a IR limit [24,25]. Figure 2(d) shows plots of  $\Gamma/\Omega$  vs  $\Omega$  for LB2 and  $d$ -SiO<sub>2</sub>. The intercept with the horizontal line at  $1/\pi$  gives  $\Omega_{\text{IR}}$ . For LB2, we find  $\hbar\Omega_{\text{IR}} \approx 8.8 \pm 0.2$  meV and  $q_{\text{IR}} \approx 2.1$  nm<sup>-1</sup>, whereas for  $d$ -SiO<sub>2</sub> one has with this criterion  $\hbar\Omega_{\text{IR}} \approx 7.0 \pm 0.2$  meV and  $q_{\text{IR}} \approx 1.8$  nm<sup>-1</sup>. In both cases  $\Omega_{\text{IR}} \approx \Omega_{\text{BP}}$  as illustrated in Fig. 3.

Although  $\Gamma/\Omega \propto \Omega^3$  in the onset of crossover, straight lines provide excellent approximations to  $\Gamma/\Omega$  vs  $\Omega$  over a relatively broad range around  $\Omega_{\text{IR}}$ , as seen in Fig. 2(d) both for LB2 and  $d$ -SiO<sub>2</sub> [26]. It is reasonable to expect that other glasses might behave similarly. Although the crossover was mostly not investigated by others, sufficient information is available in the literature to draw plots of  $\Gamma/\Omega$  and derive  $\Omega_{\text{IR}}$  for several glasses. A summary is given in Fig. 3. The vertical error bars result from the indetermination in the available  $\Gamma(\Omega)$  data. We kept in Fig. 3 *all* glasses for which these errors are reasonably

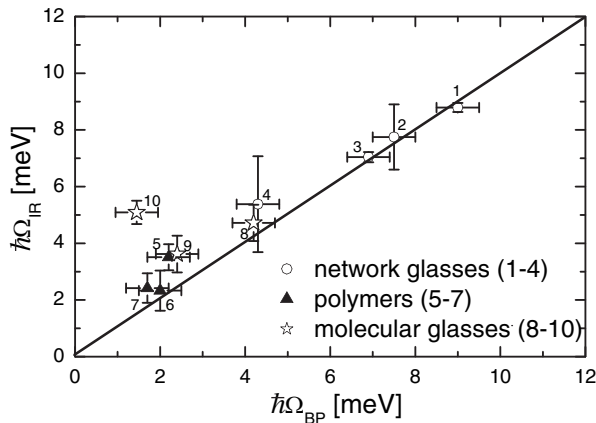


FIG. 3.  $\Omega_{\text{IR}}$  vs  $\Omega_{\text{BP}}$  for various glasses. The line  $\Omega_{\text{IR}} = \Omega_{\text{BP}}$  is a guide to the eye. The points and the references for  $\Gamma(\Omega)$  and  $\Omega_{\text{BP}}$  are (1) Li<sub>2</sub>O-2B<sub>2</sub>O<sub>3</sub>, here and [18,23]; (2) Li<sub>2</sub>O-4B<sub>2</sub>O<sub>3</sub> [18,23]; (3)  $d$ -SiO<sub>2</sub> [10,11]; (4) vitreous silica  $v$ -SiO<sub>2</sub> [14,31]; (5) polybutadiene [38,39]; (6) polycarbonate [40]; (7) Se [41,42]; (8) glycerol [43,44]; (9) ethanol [7,45]; (10) OTP [46,47].

small. For example, the information on Ca<sub>2</sub>K<sub>3</sub>(NO<sub>3</sub>)<sub>7</sub> (CKN) [27] is unfortunately insufficiently accurate to be included. The horizontal error bars, the same for all points, are a fair estimate of the inaccuracy in  $\Omega_{\text{BP}}$ . Figure 3 demonstrates that the IR crossover and the BP vibrations are closely related. Analogous considerations were already presented in [16], based on estimates of  $\Omega_{\text{IR}}$  using the soft-potential model combined with measured two-level-system parameters. Here, the same conclusion is reached based on *direct* measurements. A plausible explanation for the relation between  $\Omega_{\text{BP}}$  and  $\Omega_{\text{IR}}$  is that a bilinear coupling of quasilocal oscillators with the strain field redistributes the density of states of the former, leading to the BP [16,17]. The relation depends then on the density of oscillators and on the strength of their coupling to sound, which might vary from glass to glass. For example, ortho-terphenyl (OTP) has a very weak BP [28], so that the hybridization might not suffice to produce a clear IR crossover. This could also be the case for CKN, another very fragile glass, where crossover effects seem absent from the available data [27]. On the other hand, with our definition of  $\Omega_{\text{IR}}$ , we see from Fig. 3 that  $\Omega_{\text{IR}} \approx \Omega_{\text{BP}}$  for all sufficiently strong glasses in the Angell sense [29].

Given the general behavior of Fig. 3, one expects that the rapid growth of  $\Gamma$  below crossover should also be quite general. If so, in all sufficiently strong glasses there should be a region where  $\Gamma$  increases approximately with  $\Omega^4$ , or also with  $Q^4$  since there  $Q \propto \Omega$  [30]. Hence, the belief that there is a “universal” law  $\Gamma \propto Q^2$  in glasses [27,32] should be questioned, at least below  $\Omega_{\text{IR}}$ . To investigate this point we explored  $\Gamma$  over a larger frequency range in LB2. The results are summarized in Fig. 4 on the energy scale usually used in IXS. BLS was excited with an Ar-ion laser at 514.5 nm and analyzed with a high-resolution tandem spectrometer including a spherical Fabry-Perot interferometer as described in [33]. The Brillouin linewidth was measured as a function of the scattering angle and tem-

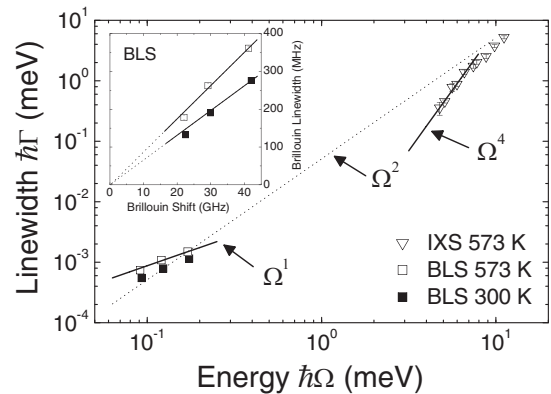


FIG. 4.  $\Gamma(\Omega)$  for LB2, showing the IXS results with the line of slope 4 from Fig. 2(b), and our own BLS measurements. The lines are guides to the eye discussed in the text. The error bars are smaller than the symbols, also in the inset.

perature. The results are illustrated for three geometries and two  $T$  values in Fig. 4, and on a more expanded linear scale in the inset. In this range we find  $\Gamma \propto \Omega$ . This, plus the temperature variation observed between 5 and 600 K, points to thermally activated relaxation as the dominant broadening mechanism [34]. The anharmonic damping contribution,  $\Gamma_{\text{anh}} \propto \Omega^2$ , can be estimated using the  $T$  dependence of the Brillouin sound velocity,  $\delta v/v = -6.5 \times 10^{-5} T(\text{K})$ , as explained in [35]. It is known that such a decrease of  $v$  is characteristic of anharmonic coupling to the thermal bath [36]. Taking as a rough estimate for the thermal-bath relaxation time that of  $d\text{-SiO}_2$  [19], we find that  $\Gamma_{\text{anh}}$  in the BLS range should be about an order of magnitude smaller than the observed  $\Gamma$ . In Fig. 4, the dotted line in  $\Omega^2$  is drawn only to point out that this interpolation between BLS and IXS results is not justified. The  $Q^2$  behavior often reported above the crossover might relate to what amounts to a strong inhomogeneous broadening as suggested in [7]. It is meaningless to extrapolate it below  $\Omega_{\text{IR}}$ .

The central result of this study, that  $\Omega_{\text{IR}} \simeq \Omega_{\text{BP}}$  in many glasses, conversely implies that the observation of a sizable BP indicates the presence of a IR crossover. One expects then  $q_{\text{IR}} \simeq \Omega_{\text{BP}}/v$ , which is always rather small. For example, in LB2, we found here that  $2\pi/q_{\text{IR}} \simeq 30 \text{ \AA}$ . A cube of that size contains over 200 formula units,  $\text{Li}_2\text{B}_4\text{O}_7$ . It is obvious that most acousticlike excitations are of shorter characteristic length, although these might be far from plane waves. A signature of such modes was actually observed in silica glass [37]. It appears on the neutron-scattering inelastic structure factor,  $S(Q, \omega)$ . The maxima in  $\omega$  of  $S(Q, \omega)$  form *pseudobranches*,  $\Omega(Q)$ . The latter are crystal-like, the peaks in the elastic structure factor  $S(Q)$  playing the role of Bragg reflections. Hence, it is not so surprising that comparing a glass to the corresponding polycrystal, acoustic measurements at very high  $Q$  give similar pseudobranches and inhomogeneous linewidths, as reported for ethanol in [7]. The glass-specific structural and dynamical properties should not be sought on the nearest neighbor scale, but rather at the nanometer scale corresponding to  $q_{\text{IR}}$ .

The authors thank A. Matic for the LB2 sample, R. Violla for recent improvements to the BLS spectrometer, and J. M. Fromental for technical assistance.

- 
- [1] R. C. Zeller and R. O. Pohl, Phys. Rev. B **4**, 2029 (1971).
  - [2] M. Rothenfusser *et al.*, Phys. Rev. B **27**, 5196 (1983).
  - [3] S. Hunklinger and W. Arnold, in *Physical Acoustics*, edited by W. P. Mason and R. N. Thurston (Academic Press, New York, 1976), Vol. XII, p. 155.
  - [4] R. Vacher *et al.*, J. Non-Cryst. Solids **45**, 397 (1981); T. C. Zhu *et al.*, Phys. Rev. B **44**, 4281 (1991).

- [5] J. E. Graebner *et al.*, Phys. Rev. B **34**, 5696 (1986).
- [6] E. Duval and A. Mermet, Phys. Rev. B **58**, 8159 (1998).
- [7] A. Matic *et al.*, Phys. Rev. Lett. **93**, 145502 (2004).
- [8] Often alluded to, e.g., in the *Encyclopedia of Materials: Science and Technology*, edited by K. H. J. Buschow *et al.* (Elsevier, Oxford, 2001), Vol. 1, articles by S. R. Elliott on pp. 171–174 and U. Buchenau on pp. 212–215.
- [9] E. Rat *et al.*, Phys. Rev. Lett. **83**, 1355 (1999).
- [10] M. Foret *et al.*, Phys. Rev. B **66**, 024204 (2002).
- [11] B. Rufflé *et al.*, Phys. Rev. Lett. **90**, 095502 (2003).
- [12] U. Buchenau *et al.*, Phys. Rev. B **34**, 5665 (1986).
- [13] S. N. Taraskin and S. R. Elliott, J. Phys. Condens. Matter **11**, A219 (1999).
- [14] B. Hehlen *et al.*, Phys. Rev. Lett. **84**, 5355 (2000).
- [15] N. V. Surotsev *et al.*, J. Phys. Condens. Matter **10**, L113 (1998).
- [16] D. A. Parshin and C. Laermans, Phys. Rev. B **63**, 132203 (2001).
- [17] V. L. Gurevich *et al.*, Phys. Rev. B **67**, 094203 (2003).
- [18] A. Matic *et al.*, Phys. Rev. Lett. **86**, 3803 (2001).
- [19] E. Rat *et al.*, Phys. Rev. B **72**, 214204 (2005).
- [20] T. Matsuo *et al.*, Solid State Ionics **154–155**, 759 (2002).
- [21] V. K. Malinovsky *et al.*, Europhys. Lett. **11**, 43 (1990).
- [22] U. Buchenau, Z. Phys. B **58**, 181 (1985).
- [23] J. Lorösch *et al.*, J. Non-Cryst. Solids **69**, 1 (1984).
- [24] A. F. Ioffe and A. R. Regel, Prog. Semicond. **4**, 237 (1960).
- [25] Our definition of the crossover is identical to that in [13] as the *amplitude* mean free path used there equals  $2\ell$ .
- [26] As the straight lines do not cross the origin, this does not imply  $\Gamma \propto \Omega^2$ .
- [27] A. Matic *et al.*, Europhys. Lett. **54**, 77 (2001).
- [28] A. P. Sokolov *et al.*, Phys. Rev. Lett. **71**, 2062 (1993).
- [29] C. A. Angell, J. Non-Cryst. Solids **131–133**, 13 (1991).
- [30] IXS data are usually not available below  $\Omega_{\text{IR}}$ , mostly for experimental reasons. For example, that the rapid onset was not evidenced in vitreous silica [31] is not indicative of its absence but rather of a low  $q_{\text{IR}} \sim 1 \text{ nm}^{-1}$ .
- [31] R. Dell’Anna *et al.*, Phys. Rev. Lett. **80**, 1236 (1998).
- [32] G. Ruocco *et al.*, Phys. Rev. Lett. **83**, 5583 (1999).
- [33] R. Vacher *et al.*, Rev. Sci. Instrum. **51**, 288 (1980).
- [34] G. Guimbretière, Ph.D. thesis, Université Montpellier 2, 2005.
- [35] R. Vacher *et al.*, Phys. Rev. B **72**, 214205 (2005).
- [36] T. N. Claytor *et al.*, Phys. Rev. B **18**, 5842 (1978).
- [37] M. Arai *et al.*, Physica (Amsterdam) **263–264B**, 268 (1999).
- [38] D. Fioretto *et al.*, Phys. Rev. E **59**, 4470 (1999).
- [39] U. Buchenau *et al.*, Phys. Rev. Lett. **77**, 4035 (1996).
- [40] J. Mattsson *et al.*, J. Phys. Condens. Matter **15**, S1259 (2003).
- [41] T. Scopigno *et al.*, Phys. Rev. Lett. **92**, 025503 (2004).
- [42] M. Foret *et al.*, Phys. Rev. Lett. **81**, 2100 (1998).
- [43] F. Sette *et al.*, Science **280**, 1550 (1998).
- [44] J. Wuttke *et al.*, Phys. Rev. E **52**, 4026 (1995).
- [45] M. A. Ramos *et al.*, Phys. Rev. Lett. **78**, 82 (1997).
- [46] G. Monaco *et al.*, Phys. Rev. Lett. **80**, 2161 (1998).
- [47] A. Tölle, Rep. Prog. Phys. **64**, 1473 (2001).